International Journal of Nanomedicine

Dovepress
open access to scientific and medical research

Open Access Full Text Article

ORIGINAL RESEARCH

Preparation, Characterization, and *Staphylococcus aureus* Biofilm Elimination Effect of Baicalein-Loaded β-Cyclodextrin-Grafted Chitosan Nanoparticles

Zhongbin Zhang[1,2,*], Jinqing Chen[1,*], Linghui Zou[1,*], Jing Tang[1], Jiaxin Zheng[1], Meijiao Luo[1], Gang Wang[1], Dan Liang[1,2], Yuyang Li[1], Ben Chen[1], Hongjun Yan[1], Wenya Ding[1–3]

[1]Guangxi University of Chinese Medicine, Nanning, People's Republic of China; [2]Key Laboratory of Common Technology of Chinese Medicine Preparations, Guangxi University of Chinese Medicine, Nanning, People's Republic of China; [3]College of Veterinary Medicine, Northeast Agricultural University, Harbin, People's Republic of China

*These authors contributed equally to this work

Correspondence: Wenya Ding, Guangxi University of Chinese Medicine, Nanning, People's Republic of China, Tel +86-15045630868, Email DingWenYa666@163.com

Background and Purpose: Infections caused by *Staphylococcus aureus* (*S. aureus*) colonization in medical implants are resistant to antibiotics due to the formation of bacterial biofilm internal. Baicalein (BA) has been confirmed as an inhibitor of bacterial biofilm with less pronounced effects owing to its poor solubility and absorption. Studies have found that β-cyclodextrin-grafted chitosan (CD-CS) can improve drug efficiency as a drug carrier. Therefore, this research aims to prepare BA-loaded CD-CS nanoparticles (CD-CS-BA-NPs) for *S. aureus* biofilm elimination enhancement.

Methods: CD-CS-BA-NPs were prepared via the ultrasonic method. The NPs were characterized using the X-ray diffraction (XRD), Thermo gravimetric analyzer (TGA), Transmission electron microscopy (TEM) and Malvern Instrument. The minimum inhibitory concentration (MIC) of the NPs were investigated. The biofilm models in vivo and in vitro were constructed to assess the *S. aureus* biofilm elimination ability of the NPs. The Confocal laser method (CLSM) and the Live/Dead kit were employed to explore the mechanism of the NPs in promoting biofilm elimination.

Results: CD-CS-BA-NPs have an average particle size of 424.5 ± 5.16 nm, a PDI of 0.2 ± 0.02, and a Zeta potential of 46.13 ± 1.62 mV. TEM images revealed that the NPs were spherical with uniform distribution. XRD and TGA analysis verified the formation and the thermal stability of the NPs. The NPs with a MIC of 12.5 ug/mL exhibited a better elimination effect on *S. aureus* biofilm both in vivo and in vitro. The mechanism study demonstrated that the NPs may permeate into the biofilm more easily, thereby improving the biofilm elimination effect of BA.

Conclusion: CD-CS-BA-NPs were successfully prepared with enhanced elimination of *S. aureus* biofilm, which may serve as a reference for future development of anti-biofilm agents.

Keywords: baicalein, β-cyclodextrin-grafted chitosan, nanoparticles, *Staphylococcus aureus*, biofilm elimination

Introduction

Staphylococcus aureus (*S. aureus*), a Gram-positive bacterium, is a leading cause of implanted medical device infections.[1,2] Under the mediation of mucins, *S. aureus* can colonize and adhere to the surface of medical implant devices, such as heart valves, deep vein catheters, urinary catheters, drainage tubes, and various diseased tissues.[3] Once attached to the surface, the bacteria begin to multiply and start secreting extracellular polysaccharides and multiplying to form biofilm, which provides *S. aureus* with a protective growth environment to resist the activity of traditional antibiotics. Bacterial biofilm refers to a cluster of bacteria with a unique three-dimensional structure[4] formed by the bacteria themselves with the proteoglycans, lipoproteins, and fibrin.[5] The mechanism of antibiotic resistance caused by biofilm lies in the following two aspects: (1) The physical barrier formed by the bacterial biofilm's unique three-dimensional structure effectively prevents the infiltration of

Received: 21 July 2022
Accepted: 25 October 2022
Published: 15 November 2022

Graphical Abstract

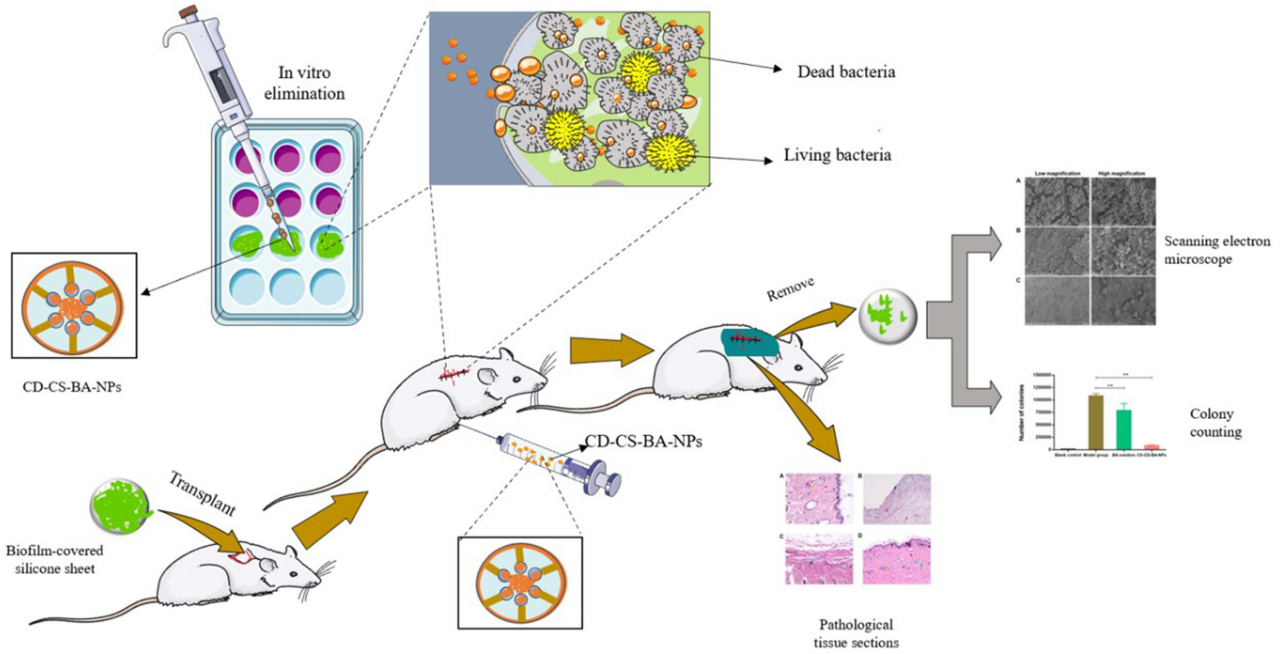

antibacterial drugs; (2) Various bacteria secrete and produce enzymes that inhibit the action of antibiotics, causing the bacteria in the biofilm to be in a hibernating state, reducing the bacteria's response ability.[6,7] These two mechanisms act synergistically and eventually lead to bacterial resistance.[8] Implantable medical devices have played an important role in clinical treatment, but they are facing the challenge of biofilm-relevant infections caused by surface-adhering bacteria, especially *S. aureus*. It is estimated that over 60% of treated bacterial infections arise from biofilm in developed countries.[9] Thus, infections of medical devices caused by *S. aureus* colonization with the formation of biofilm are becoming a common and serious problem in hospital-infected patients.[10,11] There is an urgent need to develop novel anti-biofilm formulation to overcome the drug resistance problem caused by the bacterial biofilm.

Baicalein (BA), a natural flavonoid constituent derived from the root of *Scutellaria baicalensis Georgi*, has been confirmed as a good antibacterial active ingredient that can destroy the bacterial biofilm.[12] However, its clinical applications are limited owing to its poor water solubility and absorption.[13] Early studies in our laboratory demonstrated that β-cyclodextrin-grafted chitosan (CD-CS) has good biocompatibility, stability, and antibacterial ability.[14] In addition, CD-CS can be used as a drug carrier to prepare nanoparticles for drug delivery, synergistically exerting the carrier advantages of CD and CS. Hou et al[15] have fabricated CD-CS nanoparticles using an ionic gelation method. The results showed that the CD-CS enhanced the stability, water solubility, and in vivo absorption of ketoprofen. Takechi-Haraya et al[16] pointed out that CD-CS has a markedly enhanced ability to induce cholesterol efflux from cell membranes compared to pure CD. Among them, CD has been proven to increase aqueous solubility, bioavailability, and bacterial biofilm infiltration of lipophilic drugs.[17,18] CS can extend the retention of the drug on the bacterial biofilm through charge interaction and then increase the absorption of the drug.[19] On the other hand, nanotechnology has been widely applied to improve the antibacterial efficacy and exhibited great advantages,[20] such as nanoemulsion, polymeric nanoparticles, gold nano-clusters,[21] gold nanocrystals[22]

and so on. Therefore, BA-loaded CD-CS nanoparticles (CD-CS-BA-NPs) were designed to maximize the elimination effect of BA on the bacterial biofilm.

The study was conducted by preparing CD-CS-BA-NPs, establishing the *S. aureus* biofilm models, determining the minimal inhibitory concentration (MIC) of the NPs, and investigating their elimination effect on biofilm in vivo and in vitro. Further, the CLSM was performed to examine the advantages of biofilm infiltration when CD-CS-BA-NPs were employed for drug delivery. The colony counting method and Live/Dead kit staining were used to verify the ability of the NPs to promote drug infiltration into the biofilm compared with BA solution. In addition, the possible mechanism of the NPs in biofilm elimination was preliminarily explored. The development of this research not only provides an experimental basis for the application of CD-CS-BA-NPs against the biofilm of *S. aureus* but also provides new ideas for the design of novel anti-bacteria formulations.

Materials and Methods

Materials

S. aureus (ATCC-43300) was kindly provided by the department of Animal Pharmacy, Northeast Agricultural University. SPF-grade Sprague Dawley (SD) rats (200 ± 20 g) were purchased from Hunan Slack Jing da Experimental Animal Co., Ltd. CD-CS was homemade. BA reference substances (purity: 97.9%) were obtained from the China Institute of Food and Drug Verification (Beijing, China). BA (crude drugs, purity: 95%) were purchased from Maclean Biochemical Co., Ltd. (Shanghai, China). Coumarin 6 (Calamar, purity: 98%, batch number: ZY210104). TSB medium (batch number: 1092841) was purchased from Huankai Microbial Technology Co., Ltd. (Guangdong, China) and TSA medium (batch number: 20200509) was supplied by Qingdao Hi-Tech Industrial Park Haibo Biotechnology Co., Ltd. (Qingdao, China). All other chemicals and organic solvents were of analytical grade.

Animal Studies

The animal study was approved by the Ethics Committee of the Experimental Animal Centre of Guangxi University of Chinese Medicine (Nanning, China, No. SYXK-GUI-2019-0001) and carried out in a manner consistent with the Guide for the Care and Use of Laboratory Animals. All guidelines have been strictly followed during the whole study.

Preparation of CD-CS-BA-NPs

The CD-CS-BA-NPs were prepared following a modified procedure derived from our previous publication.[23] Briefly, a standard stock solution of BA was prepared by dissolving 20 mg of BA in ethanol and making up the volume to 10 mL with ethanol to get a final BA concentration of 2 mg/mL. 2% (v/v) glacial acetic acid (5 mL) was added into a beaker with 30 mg of CD-CS. The mixture was stirred on a magnetic stirrer until completely dissolved at room temperature. One milliliter of BA stock solution was slowly added dropwise and the stirring was continued for 5 h. Thereafter, the solution was dispersed by probe sonication for 15 min (Ultrasonic cell pulverizer, VCX130; SONICS & MATERIALS Inc., USA) and then centrifuged at 4000 rpm for 10 min. The supernatant was taken out and the CD-CS-BA-NP solution was obtained eventually.

Characterization of CD-CS-BA-NPs

Particle Size and TEM Determination

One milliliter of the CD-CS-BA-NP solution was taken for the determination of the particle size and polydispersity index (PDI) using a Malvern Instrument (ZEN3700, Malvern Instruments Co., Ltd., Germany). To confirm the size measurement results and investigate the morphological characteristics of the CD-CS-BA-NPs, transmission electron microscopy (TEM; HT-7700, Hitachi, Japan) imaging was performed. An appropriate amount of the NP solution was diluted three times with pure water and then added dropwise to the copper mesh covered with carbon film. After natural drying, the microscopic appearance of the NPs was observed by the TEM.

XRD and TGA Analysis

Twenty milligram of powder samples were prepared to investigate the formation of CD-CS-BA-NPs using a X ray diffractometer (Rigaku Smart Lab SE, Tokyo, Japan) with Cu-Kα radiation. The scanning speed employed was 2°/min over a 2θ range of 5–80°. About 10 mg of samples was placed in an alumina crucible to measure the thermal stability of CD-CS-BA-NPs (TGA, Discovery TGA 550, TA Instruments, USA), and the thermal profiles were recorded from 30 to 800°C at a heating rate of 10 °C/min and an atmosphere of nitrogen.

Determination of Drug Content

The encapsulation efficiency (EE) and loading capacity (LC) were determined by slight modifications of a previously reported indirect method.[24] CD-CS-BA-NP solution (0.5 mL) was measured accurately. Absolute ethanol was added to break the NPs and get a final volume of 5 mL. The NP solution after demulsification was diluted to 5 mL with absolute ethanol and the BA content was measured by a UV spectrophotometer (UV-1900, Beijing Puxi General Instrument Co., Ltd., Beijing, China) at 276 nm. The measured value indicates the amount of BA encapsulated in the NPs and the EE was calculated according to formula (1). A gravimetric method[25] was used to determine the LC of the CD-CS-BA-NPs. Three milliliters of the NP solution and the NP solution without the addition of BA (CD-CS-NPs) were measured and placed in dry vials, respectively. The samples were freeze-dried (Christ Epsilon 2–4 vacuum freeze dryer; Martin Christ GmbH, Osterode, Germany) and weighed. The LC was calculated according to formula (2).

$$EE\ (\%)\frac{\text{Amount of BA encapsulated in nanoparticle}}{\text{Amount of initial BA}}\times 100 \tag{1}$$

$$LC\ (\%)\frac{\text{The weight difference between CD}-\text{CS}-\text{BA}-\text{NPs and CD}-\text{CS}-\text{NPs}}{\text{Weight of CD}-\text{CS}-\text{BA}-\text{NPs}}\times 100 \tag{2}$$

Solubility Study

Excessive amounts of the CD-CS-BA-NPs lyophilized powder and BA were added into the solution with different pH (1.0, 3.0, 5.0, 6.8, and 7.4). The mixture was vortexed for 30 seconds and shaken at 37°C for 48 h to reach equilibrium. These samples were then centrifuged at 13,000 rpm for 15 min, the supernatant was finally collected, and the solubility of BA was detected by the UV spectrophotometer method described above.

Establishment of *Staphylococcus aureus* Biofilm Model

S. aureus was resuscitated and cultured in agar medium conventionally until it reached the logarithmic growth phase. The bacterial solution was diluted with Tryptic soy broth (TSB) medium to get a final concentration of 1×10^6 CFU/mL. The bacterial solution was added to a 96-well microplate (100 μL per well) and incubated at 37°C. The bacterial biofilm status was assessed at 12, 18, 24, and 30 h by the crystal violet staining method.[26] Specifically, the bacterial solution was removed at different time points. Methanol (200 μL) was then added to each well for 15 min to fix the biofilm. Thereafter, 100 μL of 1% crystal violet solution was added to dye for 5 min, and the excess dye solution was washed 3 times with pure water. A 33% acetic acid (200 μL) solution was added to each well to dissolve the dye that had entered the biofilm. The microplate reader was used to measure the OD value at 595 nm to identify the optimal incubation time for the biofilm formation.

MIC Determination

The MIC of the CD-CS-BA-NPs against *S. aureus* was determined using a double dilution method.[27] Experimental groups were as follows: BA solution-treated group, CD-CS-BA-NPs-treated group, negative control group, and blank control group. The MIC was determined on the basis of the degree of clarification with naked eyes. The clarified medium in the well was regarded as having no bacteria growth. The minimum bacteria growth inhibitory drug concentration was considered as the MIC of the drug.[28]

In vitro Biofilm Elimination Studies

Crystal violet staining was performed to investigate the elimination effect of CD-CS-BA-NPs on the *S. aureus* biofilm.[29] In brief, a single colony of *S. aureus* was inoculated into TSB medium and incubated at 37°C until it reached a logarithmic phase of growth. The bacterial solution was diluted to a final concentration of 1×10^6 CFU/mL and then added into the 96-well microplate (100 μL per well) for 24 h of incubation. The bacterial solution was aspirated and CD-CS-BA-NP solution in different concentrations (125, 75, 50, and 25 μg/mL) was added. The crystal violet staining method described above was used after 12 h of incubation at 37°C to investigate the ability of the NPs in *S. aureus* biofilm elimination. On the other hand, another diluted bacteria solution (1×10^6 CFU/mL) was added to a 96-well microplate (100 μL per well) and then incubated at a constant temperature for 24 h. A CD-CS-BA-NP solution (100 μL) at a concentration of 75 μg/mL was added to the well after the bacterial solution had been aspirated. The mixture was incubated at 37°C for 3, 6, and 12 h. The OD value was measured by the crystal violet staining method described above to examine the biofilm elimination effect of the NPs for different incubation times. In addition, a colony counting method was employed to verify the inhibitory effect of the NPs on the bacteria inside the biofilm. Following the steps above until a mature biofilm was formed in the 96-well plate, the NP solution and BA solution were added, respectively. After incubation for 3 h, the biofilm was carefully scraped off and diluted with sterile saline. The sample was transferred to an EP tube and sonicated for 1.5 min in a sterile environment. The sonicated bacterial suspension was diluted 10^4, 10^6, and 10^8 times with sterile normal saline by the serial dilution method.[30] Three milliliters of the diluted bacterial suspension was poured into the agar medium (45 mL) which had been melted and cooled to 45°C. The mixture was then quickly poured into a petri dish and incubated at a constant temperature for 24 h. The number of colonies in each group visible to the naked eye was counted.[31]

In vivo Biofilm Elimination Studies

SPF-grade Sprague Dawley (SD) rats were kept in clean cages and had free access to a standard tray diet and water. All the animals had been acclimated to laboratory conditions for a week before the experiment began. A silicone sheet was placed in the 12-well plate with the bacterial solution (120 μL per well) and incubated for 24 h until it was covered with the complete biofilm. The rats were anesthetized with chloral hydrate, the back skin was shaved, and 10 mL of sterile air was injected subcutaneously into the back to form an air pouch, the biofilm-covered silicone sheets were transplanted into the subcutaneous air pouches on the backs of SD rats.[32] The rats were randomly divided into four groups: the rats in the first group were intraperitoneally injected with CD-CS-BA-NP solution at a dosage of 1.5 mg/kg; the rats in the second group were intraperitoneally injected with BA solution at a dosage of 1.5 mg/kg; the rats in the model group were injected with the same volume of saline; the rats in the blank control group were transplanted with a blank silicone sheet and treated with the same volume of saline. After being normally raised for two days, the infection of the subcutaneous tissue was observed and pathological tissue sections were prepared. Specifically, an appropriate volume (2×2×0.3 cm) of infected tissue was taken out and fixed with 4% paraformaldehyde for 24 h. The sample was dehydrated with different concentrations (80%, 90%, 95%, and 100%) of ethanol and embedded in paraffin solution. Finally, the wax block was sliced (about 4–6 μm in thickness) and stained with hematoxylin-eosin (H.E) for observation.[33] In addition, the biofilm-covered silicone sheet was taken out for colony counting to confirm the elimination effect of CD-CS-BA-NPs on the *S. aureus* biofilm. Scanning electron microscope (SEM) images were also taken to assess the microstructural changes of the biofilm. The biofilm-covered silicone sheet was removed and fixed with 2.5% glutaraldehyde-PBS solution at 4°C for 3 h. The sample was dehydrated with gradient ethanol (50%, 70%, 85%, 95%, and 100%). The microstructural changes of the biofilm were observed and photographed after gold spraying.

Mechanism of the *S. aureus* Biofilm Elimination

The CLSM was employed to investigate the infiltration of the NPs at different concentrations and incubation times. Coumarin-6, a compound that can produce fluorescence and be detected, was chosen as the model drug. Coumarin-6-loaded CD-CS nanoparticles (CD-CS-Coumarin-6-NPs) were prepared in the same way as described for CD-CS-BA-NPs. The bacteria in logarithmic growth phase were diluted to 1×10^6 CFU/mL. The diluted bacterial solution

(500 μL) was added to a sterile petri dish and incubated at a constant temperature for 24 h. After the bacterial solution was aspirated, 500 μL of the CD-CS-Coumarin-6-NPs with concentrations of 200, 140, and 80 μg/mL were added and the mixture was incubated at 37°C for 1 h. A coumarin-6 solution-treated group was set as a control group. The infiltration effect of the CD-CS-Coumarin-6-NPs with different concentrations on the *S. aureus* biofilm was observed by CLSM (Leica, Milano, Italy). In addition, 500 μL of the CD-CS-Coumarin-6-NPs (200 μg/mL) was added into another petri dish under the same conditions. The mixture was incubated at 37°C for 0.5, 1, and 3 h. The infiltration effect of CD-CS-Coumarin-6-NPs on the *S. aureus* biofilm at different incubation times was investigated similarly.

The bactericidal effect of the NPs was further verified with a Live/Dead assay kit. The bacteria in the logarithmic growth phase were diluted to 1×10^6 CFU/mL and 500 μL of the diluted bacteria solution was added to a sterile petri dish. After the mixture was incubated at a constant temperature for 24 h, the bacterial solution was aspirated. Thereafter, 500μL of CD-CS-BA-NP solution (75 μg/mL) was added into the petri dish and the mixture was incubated for 3 h. The NP solution was removed and the dish was rinsed three times with pure water. The diluted live/dead[34] staining solution (500 μL) was added to the petri dish in a dark environment. The sample was wrapped in tin foil and incubated in the dark for 15 min. The lethality of the NPs against the bacteria inside the biofilm was observed by CLSM.

Statistical Analysis

SPSS software (version 25.0) was used for statistical analysis. Data obtained in triplicate at least three times was expressed as mean ± SD. Differences between formulations were compared by a one-way analysis of variance followed by the least significant difference test; $^{**}p<0.05$ was considered significant.

Results and Discussion

Characterization of CD-CS-BA-NPs

Figure 1A schematically shows the synthesis mechanism of CD-CS-BA-NPs. As shown in Figure 1B and C, the particle size distribution of CD-CS-BA-NPs prepared by the ultrasonic method was generally uniform, and the mean particle size had already reached a nano-level of 424.5 ± 5.16 nm, which is critical to the efficacy of the nano-drug delivery system.[35] Zeta potential and PDI were 46.13 ±1.62 mV and 0.2 ± 0.02, indicating that the NPs were monodisperse and did not form aggregates.[36] The TEM images (Figure 1D) of the NPs evidenced the nanostructures with a spherical shape and showed good dispersion and uniformity, which was in good agreement with the data obtained from Malvern Instrument. The LC (%) and EE (%) of the NPs were 5.88 ± 0.69 and 73.34 ± 1.23, respectively. Cheow et al[37] noted that the higher LC and EE can improve the efficiency of treatment and reduce the dosage of drugs. From XRD images (Figure 1E), BA displayed sharp peaks, which is the characteristic of a crystalline compound. Some drug crystallinity peaks were still detectable in the physical mixture of BA and CD-CS. The diffractogram of the CD-CS-BA-NPs lyophilized product had no crystallization peak, which was in line with the curve of amorphous CD-CS. It can be speculated that BA in CD-CS-BA-NPs existed in an amorphous state, this may be helpful for solubility enhancement.[38] The TGA curves are shown in Figure 1F, an apparent thermal degradation processes about 200–301°C was observed in BA group, which was attributed to the melting of BA[39] and the weight loss below 100°C are due to water evaporation. For CD-CS, the weight reduction after 271°C might related to the decomposition of CD-CS,[40] and the weight loss in physical mixture of BA and CD-CS at 240°C might be arose from the degradation of BA and CD-CS at 240°C. In the CD-CS-BA-NPs thermogram, the thermal degradation begins at 319°C, which is higher than that of pure BA, demonstrating that the NPs had a better thermal stability. Further, it can be seen from Table 1 that the solubility of BA was significantly improved owing to the good solubilization of CD-CS. The solubility of BA gradually increased with the decrease of the buffer pH in the NPs group. The solubility of pure BA showed less change with the increasing buffer pH, and the solubility was still at a low level. Specifically, the solubility reached 262.19 ± 3.86 μg/mL at 3.0 buffer pH, this phenomenon may correspond to a previous report suggesting that chitosan would precipitate from aqueous solutions when pH increased,[41] the structure of the CD-CS may be affected to some extent and thus decreased the solubilization effect of BA.

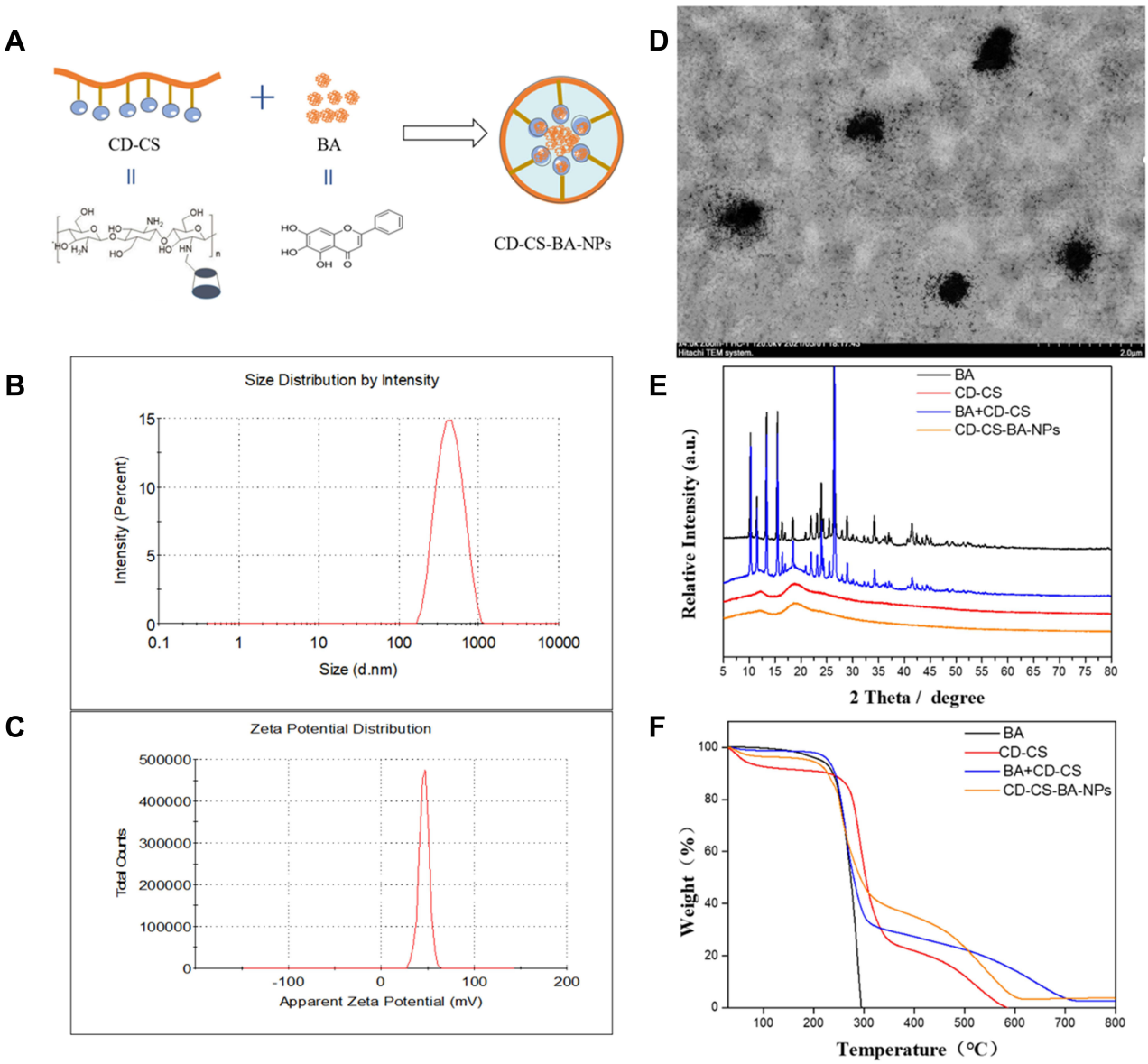

Figure 1 Synthesis mechanism of CD-CS-BA-NPs (**A**), particle size distribution (**B**), Zeta potential distribution (**C**), TEM image (**D**), XRD profiles (**E**) and TGA curves (**F**) of CD-CS-BA-NPs.

Abbreviations: TEM, transmission electron microscope; XRD, X-ray diffraction; TGA, thermo gravimetric analyzer; CD-CS-BA-NPs, baicalein-loaded β-cyclodextrin-grafted chitosan nanoparticles.

Establishment of Biofilm Model

An *S. aureus* biofilm model in vitro was established and the amount of the formed biofilm was judged by the crystal violet method.[42] The biofilm formation at different time points is presented in Figure 2. It can be seen that the OD value was visibly increased with prolonged incubation time, and the growth rate in the first 12 h was slower than that of 12–18 h. Further, the fastest growing period of the biofilm was 18–24 h, which may be related to the number of bacteria and its own reproductive characteristics. In addition, we found that the biofilm formed on the bottom of the culture plate was a membrane-like substance[43] with a slightly rough surface visible to the naked eye. The OD values has not significantly changed during 24–30 h and gradually tended to be stable after 24 h of incubation, indicating that this *S. aureus* typically forms a more mature biofilm after 24 h. This result was similar with Bauer et al that they found 24 h of incubation time were sufficient to generate a stable *S. aureus* biofilm.[44] Therefore, we chose 24 h as the modeling time for the subsequent experiments of biofilm elimination in vitro.

Table 1 Solubility of CD-CS-BA-NPs and BA at Different pH Values. (Mean ± SD, n=3)

Medium	Solubility (μg/mL)	
	CD-CS-BA-NPs	BA
pH 1.0 HCl	238.24 ± 3.86 **	2.51 ± 0.08
pH 3.0 HCl	262.19 ± 4.76 **	1.66 ± 0.61
pH 5.0 ABS	231.40 ± 8.25 **	1.87 ± 0.73
pH 6.8 PBS	225.26 ± 2.59 **	4.41 ± 0.13
pH 7.4 PBS	95.10 ± 5.29 **	10.86 ± 0.87

Note: **$p<0.05$ compared with BA.
Abbreviations: BA, baicalein; CD-CS-BA-NPs, baicalein-loaded β-cyclodextrin-grafted chitosan nanoparticles; HCl, hydrochloric acid; ABS, acetate buffer solution; PBS, phosphate buffer solution.

MIC Determination

The MIC of CD-CS-BA-NPs and BA against *S. aureus* were determined via the double dilution method. The medium in the wells where bacteria normally grow was turbid because the bacteria were suspended in the medium, and the medium tended to be clear because the growth and reproduction of the bacteria were inhibited. As shown in Table 2, the medium of CD-CS-BA-NPs-

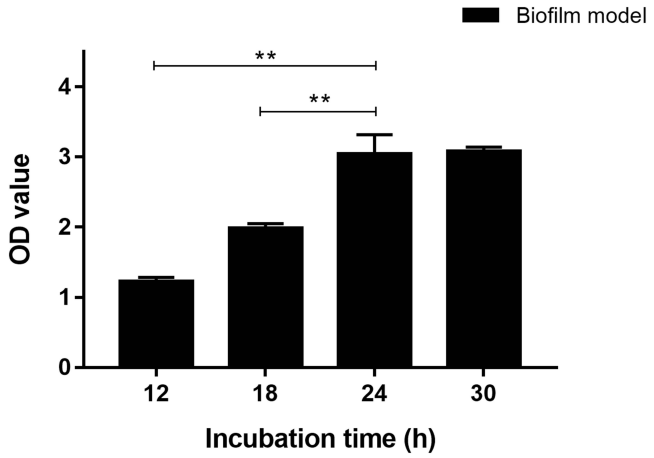

Figure 2 The maturation of *S. aureus* biofilm at different incubation times. **$p<0.05$ compared with the incubation time of 24 h.

treated group and BA solution-treated group was clear at the first four concentrations while it became turbid at the fifth concentration, demonstrating that the MIC of CD-CS-BA-NPs was 12.5 μg/mL and the MIC of BA solution was 25 μg/mL. Similar results were also reported in the study of Ma et al[45] that the MIC was decreased when curcumin was loaded in CS nanoparticles for drug delivery. The CD-CS-BA-NPs exerted antibacterial effect at a lower concentration, suggesting that the

Table 2 The MIC of CD-CS-BA-NPs and BA Against *S. Aureus*

NO.(ug/mL)	1	2	3	4	5	6	7	8	Negative Control	Blank Control
CD-CS-NPs	75	50	25	12.5	6.25	3.13	1.56	0.78	0	0
Result	-	-	-	-	+	+	+	+	+	-
BA solution	200	100	50	25	13	6	3	2	0	0
Result	-	-	-	-	+	+	+	+	+	-

Note: "-" means bacterial inhibition, the medium was clarified; "+" means normal bacterial growth, the medium was turbid.
Abbreviations: MIC, minimum inhibitory concentration; BA, baicalein; CD-CS-BA-NPs, BA-loaded β-cyclodextrin-grafted chitosan nanoparticles; *S. aureus, Staphylococcus aureus*.

antibacterial ability of BA was increased when CD-CS-BA-NPs were employed for drug delivery. This may be related to the antibacterial effect of CD-CS, as it has been reported to be capable of changing permeability of the bacterial cell membrane, exerting the antibacterial effects through membrane disruption and cell lysis.[23]

In vitro Biofilm Elimination Studies

In this experiment, we determined the elimination effect of CD-CS-BA-NPs on a mature *S. aureus* biofilm model in vitro at different concentrations (125, 75, 50, and 25 μg/mL) and incubation times (3, 6, and 12 h). The biofilm elimination results of the NPs at different concentrations are depicted in Figure 3A. The OD value of the NPs-treated group was smaller than controls at each concentration, showing the good ability to eliminate the *S. aureus* biofilm. And the inhibitory effect was significantly different ($p< 0.05$) from that of the BA group when the concentration was 25 μg/mL only. The elimination effect was enhanced with the increasing concentration of the NPs. However, the OD values of the BA solution-treated group were close to the controls at each concentration, indicating a little impact of pure BA on the bacterial biofilm. These results were in agreement with a prior study conducted by Shrestha et al[46] It can be inferred that the excellent elimination ability of the NPs may be related to the CD-CS drug carrier. From the above results, Zeta potential of the NPs was 46.13 ±1.62 mV, suggesting the NPs might have positive surface charges, which can bind to the negative charge on the surface of biofilm.[47] The charge-charge interaction between the surface of CS and *S. aureus* biofilm increased the adsorption capacity of BA. Further, the BA was enveloped in the lipophilic inner cavity of CD, which helps the BA to be better dissolved and plays the effect of biofilm elimination more effectively.

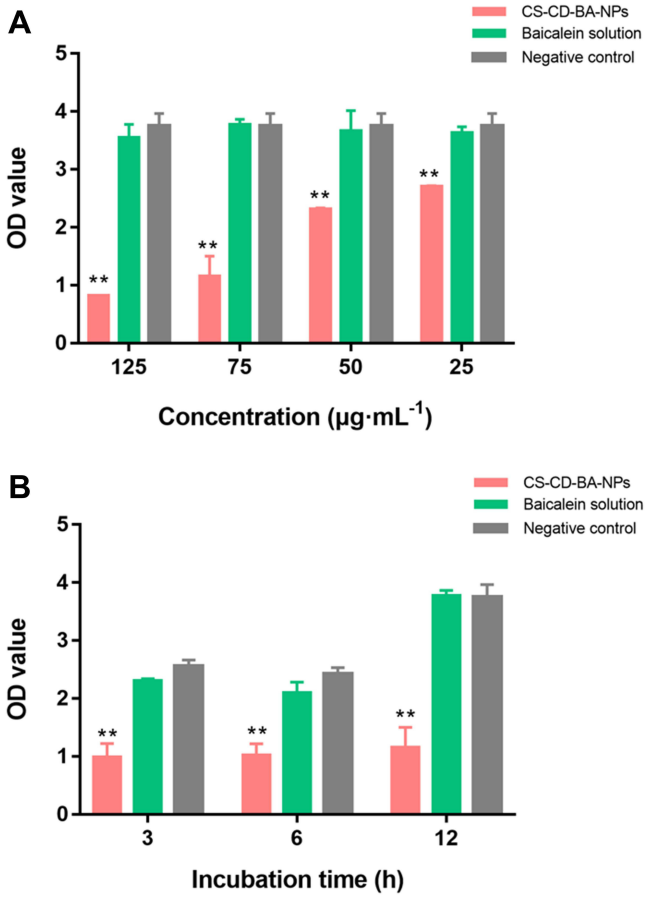

Figure 3 The elimination effect of CD-CS-BA-NPs and BA on *S. aureus* biofilm at different concentrations (**A**), and different incubation times (**B**). Untreated bacterial fluid was considered as negative control. **$p<0.05$ compared with the other group.

Abbreviations: BA, baicalein; CD-CS-BA-NPs, baicalein-loaded β-cyclodextrin-grafted chitosan nanoparticles.

On the other hand, it can be clearly seen from Figure 3B that the optimal time for biofilm elimination was 3 h in the NPs-treated group. The elimination effect was obvious compared with the BA solution-treated group, demonstrating that the BA could eliminate the biofilm more quickly when CD-CS-BA-NPs were employed for drug delivery. There was no apparent trend in the changes with the increasing co-incubation time. A possible explanation was that the NPs rapidly adhered to the bacterial biofilm, and then infiltrated into the biofilm to sterilize owing to the effect of the CD-CS, causing the amount of biofilm to no longer increase over time.[17,19,48] In this case, colony counting was used to verify the bactericidal effect of CD-CS-BA-NPs on *S. aureus*. The number of colonies was calculated and the results are shown in Figure 4. The bacterial colonies in the NPs-treated group and BA solution-treated group were significantly lower than those of the control group. And there were approximately 55 times more colonies in the BA solution-treated group compared with the NPs-treated group, indicating that CD-CS-BA-NPs had a better ability to kill the bacteria inside the biofilm, which was in agreement with the results of MIC determination that the NPs had a better antibacterial ability.

In vivo Biofilm Elimination Studies

To shed more light on the biofilm elimination effect of the CD-CS-BA-NPs, the biofilm elimination experiment in vivo was further performed. Considering that most of the medical implants such as urinary catheters[49] are made of silicone material, silicone sheet was selected as the modeling material to build the biofilm model in vivo to simulate the realistic infection conditions. Inflammation and infection were induced by transplanting the bacterial biofilm-covered silicone sheet into the subcutaneous pockets on the backs of SD rats. The difference in pathological tissue sections stained with H.E. was shown in Figure 5. The skin tissue structure of the rats in the blank group (Figure 5A) was normal with a clear layer, there was no thickening in the epidermis and the collagen fibers of the dermis were arranged neatly and tightly (red arrow); a large number of hair follicle structures were visible (yellow arrow) and there was no obvious inflammatory cell exudation. For the model group (Figure 5B), the epidermis was peeled off and the dermis was explored (black arrow); the structure of dermis was loose and edematous, and a large number of collagen fibers were missing. The inflammatory cell exudation can be observed (red arrow). The histological findings in the BA solution-treated group (Figure 5C) were consistent with the model group, the skin tissue structure was abnormal, the collagen fibers in some areas of the dermis were arranged disorderly. A small amount of inflammatory cell exudation can be seen (black arrow). In contrast, the NPs showed excellent antibacterial efficacy (Figure 5D). It can be seen that the skin tissue structure was normal and each layer structure was clear. There was no thickening in the epidermis. The collagen fibers of the dermis were arranged neatly and tightly (red arrow); a large number of hair follicle structures were visible (yellow arrow); the sebaceous gland can be observed (green arrow), and there was no obvious inflammatory cell exudation in the tissue. Thus, the NPs played an important role in the treatment of bacterial infections in vivo, especially for reducing the inflammatory exudation.

In addition, the biofilm-covered silicone sheet was removed for SEM imaging and colony counting. As shown in Figure 6, the bacterial biofilm in the model group was intact and there was a large number of bacteria. The bacteria were tightly adhered together with good morphology (Figure 6A). After being treated with BA solution, the bacterial

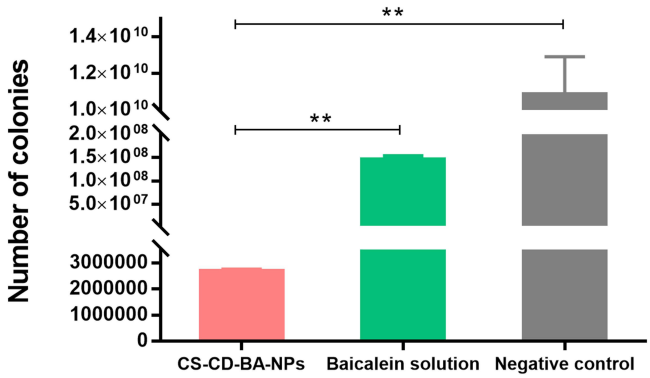

Figure 4 In vitro bactericidal effect of CD-CS-BA-NPs and BA solution on the *S. aureus* inside the biofilm was quantified by colony counting. Untreated bacterial fluid was considered as negative control. ***p*<0.05 compared with the BA solution and negative control.
Abbreviations: BA, baicalein; CD-CS-BA-NPs, baicalein-loaded β-cyclodextrin-grafted chitosan nanoparticles.

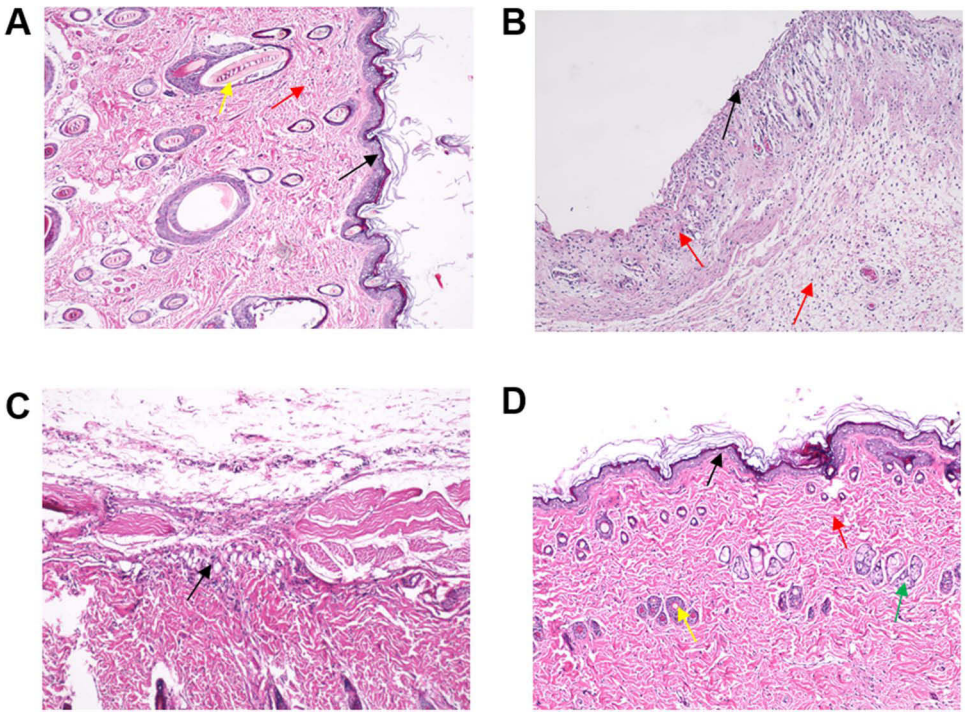

Figure 5 Pathological section analysis of inflammatory tissue around the implantation site from Blank group (**A**), Model group (**B**), BA solution-treated group (**C**), and CD-CS-BA-NPs-treated group (**D**). The red arrow refers to the collagen fibers of the dermis; The yellow arrow refers to the hair follicle structures; The black arrow refers to the inflammatory cell exudation; The green arrow refers to the sebaceous gland; Rats in blank group were implanted with blank silicone sheet and administered an equal volume of saline; Rats in model group were implanted with *S. aureus* biofilm-covered silicone sheet and administered an equal volume of saline.
Abbreviations: BA, baicalein; CD-CS-BA-NPs, baicalein-loaded β-cyclodextrin-grafted chitosan nanoparticles.

adhesions were still visible, and no significant change in the morphology of bacteria was observed (Figure 6B). It can be clearly seen that the biofilm on the silicone sheet in the NPs-treated group was more severely damaged, the adhesions and number of the bacteria were significantly decreased, the area of the biofilm was reduced, and the three-dimensional structure was obviously destroyed and cleared, demonstrating the excellent biofilm elimination ability of the CD-CS-BA-NPs. According to the in vitro biofilm elimination experiments, the elimination was quantified by crystal violet staining due to it is able to bind to the exopolysaccharide matrix in the biofilm,[50] the decrease of OD value indicated that the integrity of the biofilm was destroyed, which were matching with the observations made from SEM. On the other hand, the number of colonies on the silicone sheet in the NPs-treated group was significantly decreased compared with the BA solution-treated group and the model group (Figure 7), indicating that BA may exhibit a better bactericidal ability in vivo when CD-CS-BA-NPs were employed for drug delivery, which is generally consistent with the results of MIC determination and the pathological tissue section observations. The NPs-treated group exhibited a less severe inflammatory reaction and structural damage due to the enhanced anti-bacterial effect. A noteworthy phenomenon is that the number of colonies in each group was less than the results in vitro. Schultz et al[51] noted that the biofilm adhesions were easily disrupted due to the physical friction of the skin. This phenomenon may be related to the friction of the skin against the biofilm covered on the silicone sheet and the rats' own immune sterilization of the exposed bacteria, causing an overall decrease in the number of bacteria on the implanted biofilm-covered silicone sheet.

Mechanism of the *S. aureus* Biofilm Elimination

To clarify the advantages of CD-CS-BA-NPs for drug delivery, the CLSM was performed to determine the drug uptake by the bacteria at different formulation concentrations and incubation times. Coumarin-6 was used as a fluorescent tracker,[52] and CD-CS-Coumarin-6-NPs were prepared using the same process as the preparation of CD-CS-BA-NPs. As reported, bacteria are surrounded by a self-produced matrix of extracellular polymeric substances (EPS), which often acts as a biofilm protective barrier that prevents antimicrobial drugs from penetration, thereby protecting the bacteria cells.[53] It can be seen from Figure 8 that the NPs-treated group had a stronger green fluorescence than that of coumarin-6 solution-treated group,

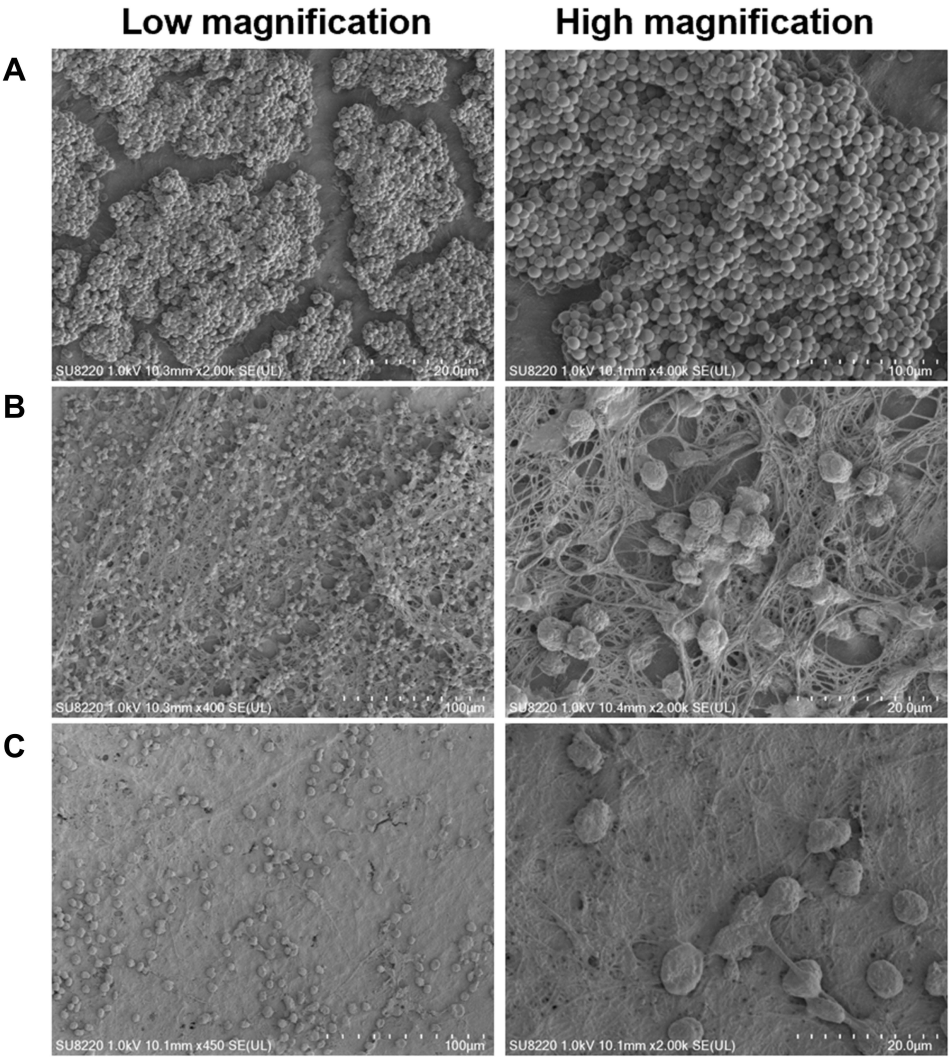

Figure 6 SEM images of the *S. aureus* biofilm covered on the silicone sheet removed from the SD rats in Model group (**A**), BA solution-treated group (**B**), CD-CS-BA-NPs-treated group (**C**). Rats in model group were implanted with *S. aureus* biofilm-covered silicone sheet and administered an equal volume of saline; SEM, scanning electron microscopy.

Abbreviations: BA, baicalein; CD-CS-BA-NPs, baicalein-loaded β-cyclodextrin-grafted chitosan nanoparticles.

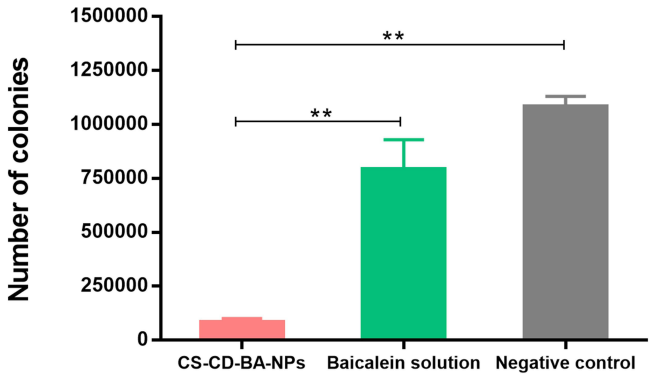

Figure 7 In vivo colony counting results of the *S. aureus* inside the biofilm on the implanted silicone after intraperitoneal injection of CD-CS-BA-NPs and BA solution for two days. Saline-treated group was used as a negative control.

Abbreviations: BA, baicalein; CD-CS-BA-NPs, baicalein-loaded β-cyclodextrin-grafted chitosan nanoparticles; $^{**}p<0.05$ compared with the BA solution and negative control.

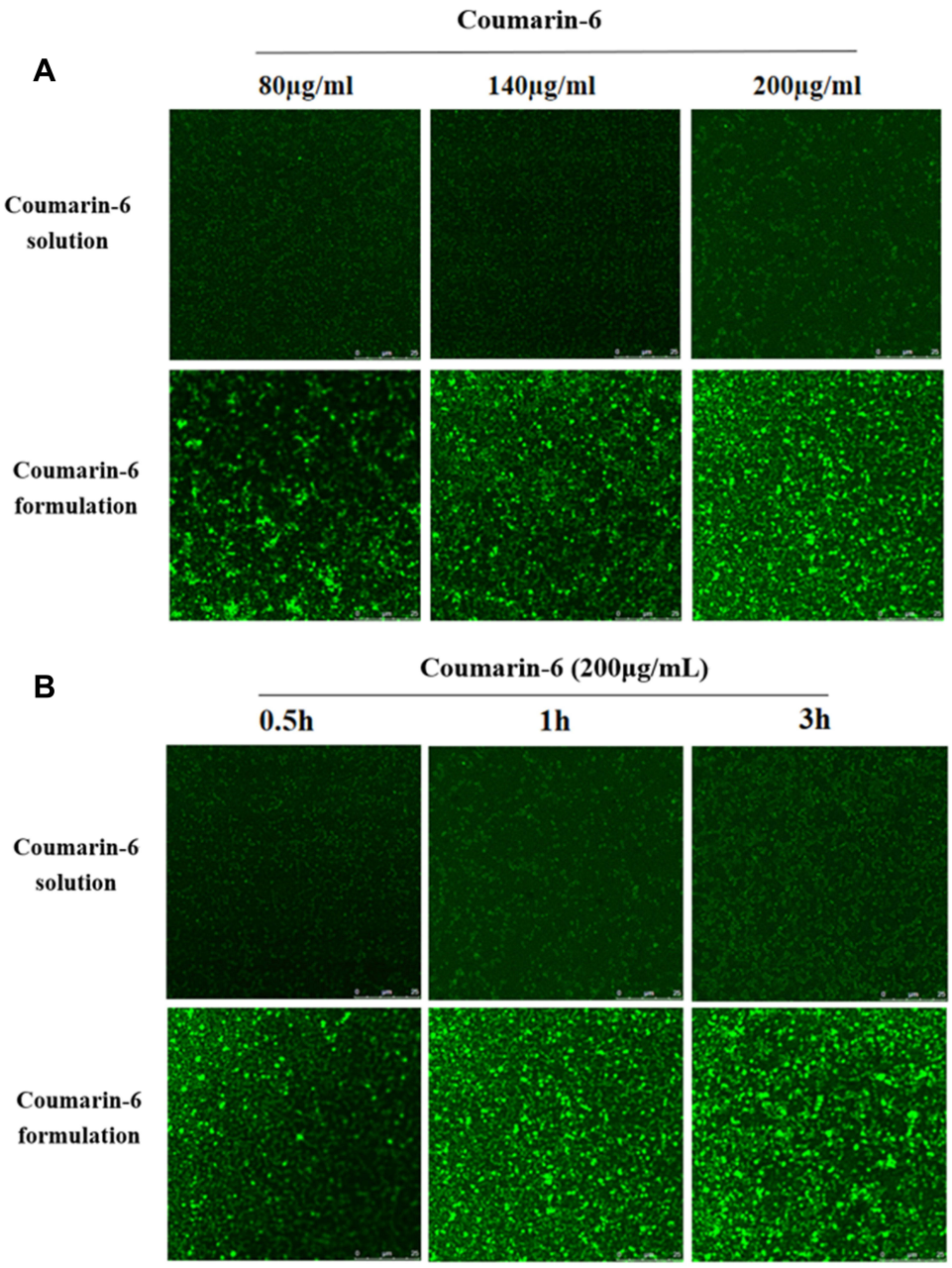

Figure 8 Infiltration effect of CD-CS-Coumarin-6-NPs and Coumarin-6 solution on *S. aureus* biofilm at different concentration (**A**) and different incubation times (**B**) were detected by CLSM.
Abbreviations: CD-CS-Coumarin-6-NPs, Coumarin-6-loaded β-cyclodextrin-grafted chitosan nanoparticles; CLSM, confocal laser microscopy.

demonstrating that more coumarin-6 permeated into the EPS when loaded in CD-CS-Coumarin-6-NPs. This result may also explain the greater effect of the CD-CS-BA-NPs on the biofilm elimination due to the better permeability. Further, the fluorescent tissue tends to be more brightly colored with increasing incubation time and formulation concentration, indicating that more coumarin-6 permeate was infiltrated into the biofilm, this concentration- and incubation time-dependent manner was in agreement with the in vitro biofilm elimination studies. On the other hand, to verify the better biofilm infiltration effect of the NPs, a Live/Dead kit was used to evaluate the bactericidal effect of the NPs after infiltration, in which green fluorescence indicated live bacteria and red fluorescence indicated dead bacteria (Figure 9). The decrease of live bacteria in the CD-CS-BA-NPs-treated group can be visualized in the contrast between Figure 9A and B, the ratio of living bacteria and dead bacteria was decreased apparently after treatment of CD-CS-BA-NPs (Figure 9C), which is

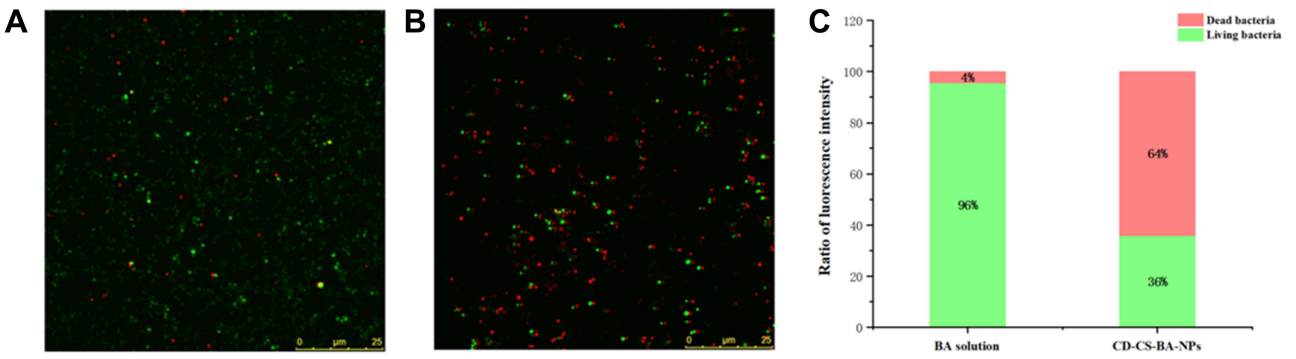

Figure 9 Bactericidal effect of BA solution (**A**) and CD-CS-BA-NPs (**B**) against *S. aureus* inside the biofilm was verified by Live/Dead assay kit. The ratio of fluorescence intensity of living and dead bacteria (**C**).
Abbreviations: BA, baicalein; CD-CS-BA-NPs, baicalein-loaded β-cyclodextrin-grafted chitosan nanoparticles; Green fluorescence represents living bacteria, and red fluorescence indicates dead bacteria.

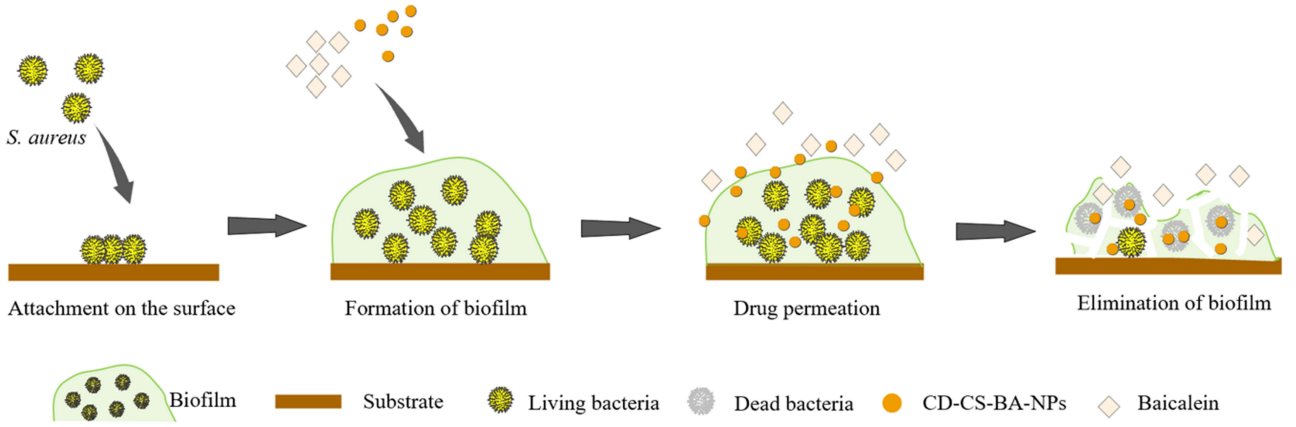

Figure 10 Schematic diagram of the biofilm elimination mechanism.

consistent with the results of the colony counting results. CS has been reported to be a cationic polymer with bio-adhesive properties, which can increase the retention of drugs in biofilm, and its positively charged groups can also interact with negative charges on the biofilm surface to enhance the permeability of the biofilm.[54] In addition, the rim of CD is hydrophilic and the cavity is hydrophobic, so it can provide a hydrophobic binding site like an enzyme or as an encapsulation of various hydrophobic drugs such as BA.[55] And it has been reported that the particle size of nanoparticles range 5 to 500 nm can pass through EPS. Thus, CD-CS-BA-NPs with a particle size of 424.5 ± 5.16 nm prepared in this study may permeate into the biofilm more effectively.[56] The permeation effect presented here (Figure 10) may be one of the possible manifestations of the previous speculation that more BA could be adsorbed on the surface of the *S. aureus* biofilm when CD-CS-BA-NPs were employed for drug delivery. After infiltrated into the biofilm, BA could better exert its bactericidal effects as shown in the results of the Live/Dead kit experiment.

Conclusion

CD-CS-BA-NPs with good physicochemical properties were successfully prepared and proved to be effective for enhancing the effect of BA on *S. aureus* biofilm elimination. The CD-CS-BA-NPs fabricated here is a promising drug delivery system for eliminating bacterial biofilm, which provides new ideas for the development of novel antibacterial formulations.

Acknowledgments

This research was supported by the National Natural Science Foundation of China (No.82060806), China Postdoctoral Science Foundation (2019M661246), Graduate education innovation program of Guangxi University of Chinese Medicine

(YCSZ2022008), Research and training project of college students in Guangxi University of Chinese Medicine (2021DXS09) and Qihuang High-level Talent Team Cultivation Project of Guangxi University of Chinese Medicine (2021002).

Disclosure

The authors report no conflicts of interest in this work.

References

1. Johnson WL, France DC, Rentz NS, et al. Sensing bacterial vibrations and early response to antibiotics with phase noise of a resonant crystal. *Sci Rep*. 2017;7(1):12138. doi:10.1038/s41598-017-12063-6
2. Nouri F, Karami P, Zarei O, et al. Prevalence of common nosocomial infections and evaluation of antibiotic resistance patterns in patients with secondary infections in Hamadan, Iran. *Infect Drug Resist*. 2020;13:2365. doi:10.2147/IDR.S259252
3. Khatoon Z, McTiernan CD, Suuronen EJ, et al. Bacterial biofilm formation on implantable devices and approaches to its treatment and prevention. *Heliyon*. 2018;4(12):e01067. doi:10.1016/j.heliyon.2018.e01067
4. Watnick P, Kolter R. Biofilm, city of microbes. *J Bacteriol*. 2000;182(10):2675–2679. doi:10.1128/JB.182.10.2675-2679.2000
5. Gómez-Gómez JM, Amils R. Crowning: a novel Escherichia coli colonizing behaviour generating a self-organized Corona. *BMC Res Notes*. 2014;7:108.
6. Xiu W, Shan J, Yang K, et al. Recent development of nanomedicine for the treatment of bacterial biofilm infections. *View*. 2021;2(1):20200065.
7. Williamson KS, Richards LA, Perez-Osorio AC, et al. Heterogeneity in Pseudomonas aeruginosa biofilms includes expression of ribosome hibernation factors in the antibiotic-tolerant subpopulation and hypoxia-induced stress response in the metabolically active population. *J Bacteriol*. 2012;194(8):2062–2073.
8. Singh S, Singh SK, Chowdhury I, et al. Understanding the mechanism of bacterial biofilms resistance to antimicrobial agents. *Open Microbiol J*. 2017;11:53–62.
9. Guo H, Tong Y, Cheng J, et al. Biofilm and small colony variants—an update on staphylococcus aureus strategies toward drug resistance. *Int J Mol Sci*. 2022;23(3):1241.
10. Ampofo EK, Amponsah IK, Asante-Kwatia E, et al. Indigenous medicinal plants as biofilm inhibitors for the mitigation of antimicrobial resistance. *Adv Pharmacol Pharm Sci*. 2020;2020:8821905. doi:10.1155/2020/8821905
11. Yougbaré S, Mutalik C, Okoro G, et al. Emerging trends in nanomaterials for antibacterial applications. *Int J Nanomed*. 2021;16:5831. doi:10.2147/IJN.S328767
12. Chen Y, Liu T, Wang K, et al. Baicalein inhibits *Staphylococcus aureus* biofilm formation and the quorum sensing system in vitro. *PLoS One*. 2016;11(4):e0153468. doi:10.1371/journal.pone.0153468
13. Wu H, Liu Z, Peng J, et al. Design and evaluation of baicalin-containing in situ pH-triggered gelling system for sustained ophthalmic drug delivery. *Int J Pharm*. 2011;410(1–2):31–40. doi:10.1016/j.ijpharm.2011.03.007
14. Ding W, Sun J, Lian H, et al. The influence of shuttle-shape emodin nanoparticles on the Streptococcus suis biofilm. *Front Pharmacol*. 2018;9:227. doi:10.3389/fphar.2018.00227
15. Hou X, Zhang W, He M, et al. Preparation and characterization of β-cyclodextrin grafted N-maleoyl chitosan nanoparticles for drug delivery. *Asian J Pharm Sci*. 2017;12(6):558–568. doi:10.1016/j.ajps.2017.07.007
16. Takechi-Haraya Y, Tanaka K, Tsuji K, et al. Molecular complex composed of β-cyclodextrin-grafted Chitosan and pH-sensitive amphipathic peptide for enhancing cellular cholesterol efflux under acidic pH. *Bioconjug Chem*. 2015;26(3):572–581. doi:10.1021/acs.bioconjchem.5b00037
17. Zhou Q, Zhong L, Wei X, et al. Baicalein and hydroxypropyl-γ-cyclodextrin complex in poloxamer thermal sensitive hydrogel for vaginal administration. *Int J Pharm*. 2013;454(1):125–134. doi:10.1016/j.ijpharm.2013.07.006
18. Aiassa V, Zoppi A, Becerra MC, et al. Enhanced inhibition of bacterial biofilm formation and reduced leukocyte toxicity by chloramphenicol: β-cyclodextrin: n-acetylcysteine complex. *Carbohydr Polym*. 2016;152:672–678. doi:10.1016/j.carbpol.2016.07.013
19. Hu F, Zhou Z, Xu Q, et al. A novel pH-responsive quaternary ammonium chitosan-liposome nanoparticles for periodontal treatment. *Int J Biol Macromol*. 2019;129:1113–1119. doi:10.1016/j.ijbiomac.2018.09.057
20. Yin Y, Hu B, Yuan X, et al. Nanogel: a versatile nano-delivery system for biomedical applications. *Pharmaceutics*. 2020;12(3):290. doi:10.3390/pharmaceutics12030290
21. Kuo JC, Tan SH, Hsiao YC, et al. Unveiling the antibacterial mechanism of gold nanoclusters via in situ transmission electron microscopy. *ACS Sustainable Chem Eng*. 2021;10(1):464–471. doi:10.1021/acssuschemeng.1c06714
22. Yougbaré S, Chou HL, Yang CH, et al. Facet-dependent gold nanocrystals for effective photothermal killing of bacteria. *J Hazard Mater*. 2021;407:124617. doi:10.1016/j.jhazmat.2020.124617
23. Ding W, Zheng S, Qin Y, et al. Chitosan grafted with β-cyclodextrin: synthesis, characterization, antimicrobial activity, and role as absorbefacient and solubilizer. *Front Chem*. 2019;6:657. doi:10.3389/fchem.2018.00657
24. Ngampunwetchakul L, Toonkaew S, Supaphol P, et al. Semi-solid poly (vinyl alcohol) hydrogels containing ginger essential oil encapsulated in chitosan nanoparticles for use in wound management. *J Polym Res*. 2019;26(9):224. doi:10.1007/s10965-019-1880-8
25. Khodaverdi E, Honarmandi R, Alibolandi M, et al. Evaluation of synthetic zeolites as oral delivery vehicle for anti-inflammatory drugs. *Iran J Basic Med Sci*. 2014;17(5):337.
26. Bendouah Z, Barbeau J, Hamad WA, et al. Biofilm formation by staphylococcus aureus and pseudomonas aeruginosa is associated with an unfavorable evolution after surgery for chronic sinusitis and nasal polyposis. *Otolaryngol Head Neck Surg*. 2006;134(6):991–996. doi:10.1016/j.otohns.2006.03.001
27. Song R, Yan F, Cheng M, et al. Ultrasound-assisted preparation of exopolysaccharide/nystatin nanoemulsion for treatment of vulvovaginal candidiasis. *Int J Nanomed*. 2020;15:2027. doi:10.2147/IJN.S241134
28. Tan S, Gao J, Li Q, et al. Synergistic effect of chlorogenic acid and levofloxacin against Klebsiella pneumonia infection in vitro and in vivo. *Sci Rep*. 2020;10(1):20013. doi:10.1038/s41598-020-76895-5

29. Kelly D, McAuliffe O, Ross RP, et al. Prevention of Staphylococcus aureus biofilm formation and reduction in established biofilm density using a combination of phage K and modified derivatives. *Lett Appl Microbiol*. 2012;54(4):286–291. doi:10.1111/j.1472-765X.2012.03205.x
30. Cotter PA, Miller JF. BvgAS-mediated signal transduction: analysis of phase-locked regulatory mutants of Bordetella bronchiseptica in a rabbit model. *Infect Immun*. 1994;62(8):3381–3390. doi:10.1128/iai.62.8.3381-3390.1994
31. Khoshnoudi-Nia S, Moosavi-Nasab M, Nassiri SM, et al. Determination of total viable count in rainbow-trout fish fillets based on hyperspectral imaging system and different variable selection and extraction of reference data methods. *Food Anal Methods*. 2018;11(12):3481–3494. doi:10.1007/s12161-018-1320-0
32. Kofuji K, Ito T, Murata Y, et al. Effect of chondroitin sulfate on the biodegradation and drug release of chitosan gel beads in subcutaneous air pouches of mice. *Biol Pharm Bull*. 2002;25(2):268–271. doi:10.1248/bpb.25.268
33. Wang Y, Wang N, Cui L, et al. Long non-coding RNA MEG3 alleviated ulcerative colitis through upregulating miR-98-5p-sponged IL-10. *Inflammation*. 2021;44(3):1049–1059. doi:10.1007/s10753-020-01400-z
34. Wang H, Qi J, Dong Y, et al. Characterization of attachment and biofilm formation by meat-borne Enterobacteriaceae strains associated with spoilage. *LWT*. 2017;86:399–407. doi:10.1016/j.lwt.2017.08.025
35. Gan Q, Wang T, Cochrane C, et al. Modulation of surface charge, particle size and morphological properties of chitosan–TPP nanoparticles intended for gene delivery. *Colloids Surf B Biointerfaces*. 2005;44:65–73. doi:10.1016/j.colsurfb.2005.06.001
36. Suchyta DJ, Schoenfisch MH. Controlled release of nitric oxide from liposomes. *ACS Biomater Sci Eng*. 2017;3(9):2136–2143. doi:10.1021/acsbiomaterials.7b00255
37. Cheow WS, Hadinoto K. Enhancing encapsulation efficiency of highly water-soluble antibiotic in poly (lactic-co-glycolic acid) nanoparticles: modifications of standard nanoparticle preparation methods. *Colloids Surf A*. 2010;370(1–3):79–86. doi:10.1016/j.colsurfa.2010.08.050
38. Tong M, Wu X, Zhang S, et al. Application of TPGS as an efflux inhibitor and a plasticizer in baicalein solid dispersion. *Eur J Pharm Sci*. 2022;168:106071. doi:10.1016/j.ejps.2021.106071
39. Hu X, Wang X, Han L, et al. Antioxidant and antimicrobial polyvinyl alcohol electrospun nanofibers containing baicalein-hydroxypropyl-β-cyclodextrin inclusion complex. *Colloids Surf A*. 2021;614:126135. doi:10.1016/j.colsurfa.2021.126135
40. Esmaeilzadeh M, Sadjadi S, Salehi Z. Pd immobilized on hybrid of magnetic graphene quantum dots and cyclodextrin decorated chitosan: an efficient hydrogenation catalyst. *Int J Biol Macromol*. 2020;150:441–448. doi:10.1016/j.ijbiomac.2020.02.094
41. Sogias IA, Khutoryanskiy VV, Williams AC. Exploring the factors affecting the solubility of chitosan in water. *Macromol Chem Phys*. 2010;211(4):426–433. doi:10.1002/macp.200900385
42. Ommen P, Zobek N, Meyer RL. Quantification of biofilm biomass by staining: non-toxic safranin can replace the popular crystal violet. *J Microbiol Methods*. 2017;141:87–89. doi:10.1016/j.mimet.2017.08.003
43. Smith K, Perez A, Ramage G, et al. Biofilm formation by Scottish clinical isolates of Staphylococcus aureus. *J Med Microbiol*. 2008;57(8):1018–1023.
44. Bauer J, Siala W, Tulkens PM, et al. A combined pharmacodynamic quantitative and qualitative model reveals the potent activity of daptomycin and delafloxacin against Staphylococcus aureus biofilms. *Antimicrob Agents Chemother*. 2013;57(6):2726–2737.
45. Ma S, Moser D, Han F, et al. Preparation and antibiofilm studies of curcumin loaded chitosan nanoparticles against polymicrobial biofilms of Candida albicans and Staphylococcus aureus. *Carbohydr Polym*. 2020;241:116254.
46. Shrestha A, Hamblin MR, Kishen A. Photoactivated rose bengal functionalized chitosan nanoparticles produce antibacterial/biofilm activity and stabilize dentin-collagen. *Nanomedicine*. 2014;10(3):491–501.
47. Horev B, Klein MI, Hwang G, et al. pH-activated nanoparticles for controlled topical delivery of farnesol to disrupt oral biofilm virulence. *ACS Nano*. 2015;9(3):2390–2404.
48. Qiao Z, Yao Y, Song S, et al. Silver nanoparticles with pH induced surface charge switchable properties for antibacterial and antibiofilm applications. *J Mater Chem B*. 2019;7(5):830–840.
49. Lawrence EL, Turner IG. Materials for urinary catheters: a review of their history and development in the UK. *Med Eng Phys*. 2005;27(6):443–453.
50. De Zoysa GH, Wang K, Lu J, et al. Covalently immobilized battacin lipopeptide gels with activity against bacterial biofilms. *Molecules*. 2020;25(24):5945.
51. Schultz MP, Walker JM, Steppe CN, et al. Impact of diatomaceous biofilms on the frictional drag of fouling-release coatings. *Biofouling*. 2015;31(9–10):759–773.
52. Finke JH, Richter C, Gothsch T, et al. Coumarin 6 as a fluorescent model drug: how to identify properties of lipid colloidal drug delivery systems via fluorescence spectroscopy? *Eur J Lipid Sci Technol*. 2014;116(9):1234–1246.
53. Hassan D, Omolo CA, Fasiku VO, et al. Formulation of pH-responsive quatsomes from quaternary bicephalic surfactants and cholesterol for enhanced delivery of vancomycin against methicillin resistant Staphylococcus aureus. *Pharmaceutics*. 2020;12(11):1093.
54. Zhu X, Chen X, Jia Z, et al. Cationic chitosan@ Ruthenium dioxide hybrid nanozymes for photothermal therapy enhancing ROS-mediated eradicating multidrug resistant bacterial infection. *J Colloid Interface Sci*. 2021;603:615–632.
55. Tom L, Nirmal CR, Dusthackeer A, et al. Formulation and evaluation of β-cyclodextrin-mediated inclusion complexes of isoniazid scaffolds: molecular docking and in vitro assessment of antitubercular properties. *New J Chem*. 2020;44(11):4467–4477.
56. Liu Y, Shi L, Su L, et al. Nanotechnology-based antimicrobials and delivery systems for biofilm-infection control. *Chem Soc Rev*. 2019;48(2):428–446.